Combustion oscillations in gas fired appliances: Eigen-frequencies and stability regimes

M. Elsari, A. Cummings*

Department of Engineering, University of Hull, Cottingham Road, Hull HU6 7RX, UK

Abstract

This paper presents a one-dimensional acoustic model for prediction of the frequencies of self-excited oscillation and acoustic mode shapes in combustion systems. The impedance of the combustion system is represented in terms of a frequency response function (FRF). Impedances of the settling and combustion chambers are predicted by using the acoustic model, taking into account the temperature distribution in the combustion chamber. Reasonably good agreement between measured and predicted acoustic resonance frequencies and mode shapes was achieved. Some data on stability regimes are discussed.
© 2003 Elsevier Science Ltd. All rights reserved.

Keywords: Combustion; Instability; Eigen-frequencies; Prediction; Measurement

1. Introduction

Higgins [1] appears to have been the first to report combustion instabilities in the literature. He observed that a ducted flame produced oscillatory noise for certain lengths of the fuel supply line. The frequency of the tone was near that of one of the longitudinal acoustic modes of the tube. The occurrence of the "singing", the mode order and the amplitude depend on the thermal diffusivity and heating value of the fuel, the fuel supply rate, the configuration of the fuel supply line and the dimensions of the combustion tube [2]. This type of combustion oscillation is sometimes known as the "singing flame" phenomenon and has been studied by many authors. Rayleigh [3] proposed a criterion for the occurrence of combustion instabilities and

---

* Corresponding author. Tel.: +44-1482-465069; fax: +44-1482-466664.
 E-mail address: a.cummings@hull.ac.uk (A. Cummings).

presented an analysis of the singing flame experiment. More generally, oscillations may be of the longitudinal, radial or tangential type [4]. Besides these simple modes, there are also mixed modes with the characteristics of all three, each having its discrete natural frequency [5]. They have been observed in industrial burners such as residential heaters [4] and also in jet engine afterburners [6], ramjets and rockets. Tsuji and Takeno [7], for example, investigated combustion oscillations in a research rocket combustor. They plotted instability regimes in terms of parameters such as fuel/oxidant equivalence ratio and combustion chamber length. A sizable number of publications exists concerning combustion instability in gas-fired burners, and in industrial and domestic gas and oil-fired systems. In applications such as central heating boilers, the occurrence of combustion driven instabilities is much more problematic than turbulence-induced combustion noise because of the higher acoustic amplitude. In some cases combustion-driven oscillations are not necessarily undesirable, however. In pulse combustors, combustion oscillations are actually necessary to the functioning of these devices. By enhancing mixing, they can increase combustion efficiency and reduce pollutant levels [8].

Schimmer and Vortmeyer [9], in a study of combustion oscillations in a laboratory combustion system (similar to that employed by Putnam and Dennis [10]), also obtained an instability plot in the plane of equivalence ratio and oscillation period, comparable to that obtained by Tsuji and Takeno [7]. They found that a change of sign of the reactance (imaginary part of impedance at the burner surface) occurred exactly at the maximum frequency of oscillation. By analogy to electrical transmission line theory, they define ''inductive'' and ''capacitive'' burner reactances. Oscillations were only observed for an inductive burner reactance. Schimmer and Vortmeyer discussed two possible driving mechanisms: (1) pulsating feed supply, and (2) pulsating laminar flame speed caused by oscillating heat transfer to the flame holder. Janardan et al. [11] measured the cold combustor admittance by using a modified impedance tube technique to investigate the driving of rocket combustor oscillations by gaseous propellant injectors. They found that the injectors could sustain combustion instabilities over a wide range of frequencies and injector design parameters. In addition, the driving characteristics of the injectors were found to depend on the propellant equivalence ratio. Chen and Chen [12] applied the approach of direct acoustic admittance measurement to investigate and elucidate the close relations between sound emission, cold burner acoustic admittance, flame equivalence ratio and combustor length. The admittance data were obtained by directly measuring the amplitudes of velocity and pressure oscillations, and the phase relations between the oscillatory velocity and pressure. They found that the flame parameters are important in determining the strength of possible sound emission. Mugridge [13] derived an equation (based on energy considerations) for combustion driven oscillations caused by a planar flame in a tube. The equation included acoustic impedances on either side of the combustion zone, a transfer function defining the response of the flame to velocity oscillations and loss of acoustic energy due to sound emission from open ends. The results in [13] indicate that the flame transfer function plays a dominant role in determining

the acoustic stability of the cavity and that Merk's [14] transfer function is not adequate for describing the occurrence of oscillations in the experimental combustion system.

In short, a universal model for predicting combustion instabilities does not exist and a complete solution to the problem can hardly be achieved given the current state of knowledge. Useful results can, however, still be achieved if fundamental studies are carried out on simplified systems, complemented by more practical investigations. The current research is a part of a larger study of the use of passive devices in the control of combustion oscillations. It is aimed not at the prediction of instability regimes, but—in a more practical sense—at the suppression of instabilities. A simple one-dimensional model of the acoustics of an experimental combustion system is used to predict the frequency of oscillations of the system. This model also can predict the sound pressure pattern in the combustion system and is a useful design tool, aiding in the location of the correct position of passive devices in the combustion system. The predictive model is described here and experimental data are compared to numerical predictions. Some measured data on instability regimes are also given.

2. Experimental combustion system

Investigations of combustion instability were performed by using a combustion system of simple geometry, similar in principle to those used by previous authors (see Putnam and Dennis [10] and Chen and Chen [12]. The combustion system used in this research is shown in Fig. 1. The term "combustion system" is used to designate the whole system between the inlet to the supply system and the flue outlet. The combustion system is divided into a supply system, a burner section, a combustion chamber and a flue. The supply system is defined as the system through which the unburned gases flow, and may be subdivided into the "silencer" and the settling chamber. The silencer is intended to act as a definable upstream acoustic termination in the air/fuel supply system. The burner section is the device on which the flames are stabilised; its principal part is the perforated burner head. The combustion chamber is defined as the section through which the combustion products flow.

The air and gas are injected into the mixing tube. The air enters this at one end, while the gas is fed in along the axis through a smaller pipe. The mixture then flows first into the silencer and then into the settling chamber, from which it passes through the burner head. The mixture is burned at the burner head and the flue gases flow through the combustion chamber and finally to the flue exit.

The silencer section consisted of a cylindrical shell 79 cm long and 9.5 cm in diameter. A 21 mm diameter wire mesh tube separated the outer layer of acoustic absorbent (glass fibre blanket) from the central gas flow passage. The silencer connected the mixing tube to the settling chamber. The settling chamber consisted of a number of rectangular duct sections of different lengths and 20×20 cm^2 internal cross-section. This design allowed the chamber height to be systematically varied from 5 cm to 45 cm. The bottom section was mounted on a concrete block. A blow-
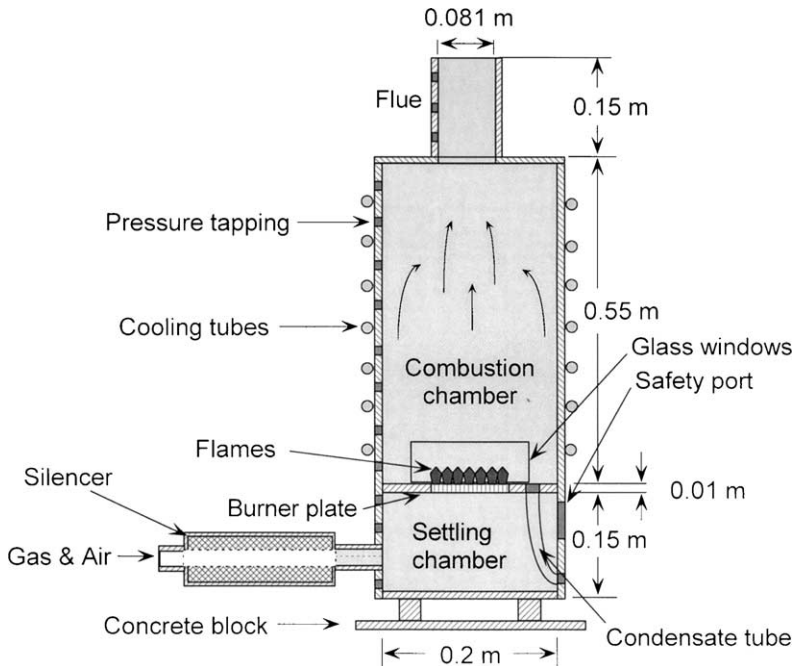
Fig. 1. A schematic of the combustion system (not to scale).

out port in the bottom of the settling chamber was made in order to release any excess pressure caused by ignition. The burner section was located between the settling chamber and the combustion chamber. The burner plate measured 20×20 cm^2 and was 10 mm thick; it was fitted in the centre of the burner section. A 10 mm hole was drilled in the burner plate and connected to a plastic tube, passing through the settling chamber, to remove the condensation. The burner head was made of steel plate, 0.75 mm thick and 11.3×9.2 cm, perforated by 2058 holes of 0.77 mm diameter, and was fitted in the centre of the burner plate. The combustion chamber was of sectional construction, which was similar to that of the settling chamber. Its height could be varied from 5 cm to 77.5 cm. The outer walls of the combustion chamber sections were surrounded by copper cooling pipes, in good thermal contact with the outer walls of the sections, to cool the combustion chamber and prevent heat damage during the operation of the burner. An additional cylindrical duct of 81 mm diameter was attached to the centre of a flat plate to cover the top of the combustion chamber and to act as the exhaust flue for the burner. In the walls of the combustion chamber was a series of 10 mm diameter access ports that could be sealed by mild steel plugs when not in use. These ports permitted the insertion, into the combustion chamber, of a water-cooled probe microphone (for detection of the sound pressure) or a suction pyrometer (for measurement of the temperature distribution). A rectangular glass window was fitted in the wall of the combustion chamber to enable the flames to be observed during ignition and operation of the burner.

3. A simple model for the acoustics of the system

In this section, a one-dimensional model of the acoustics of the combustion system will be described. Fig. 2 is a schematic diagram of the flame zone, in which the gas increases in temperature from "cold" to "hot".

In the development of the model, the following assumptions will be made:

   i. The mean flow Mach number of the combustible mixture is small, i.e. the flow velocity is negligible when compared to the local speed of sound.
  ii. Only plane waves will be assumed to propagate along the duct.
 iii. The length of the flame is assumed to be small compared to the acoustic wavelength so that the region of steady heat release may be approximated as a thin layer located at an equilibrium position of $x = 0$.
  iv. Entropy fluctuations have not been explicitly taken into account and the flame has been represented as a harmonic monopole source, of radian frequency ω and volume velocity/unit cross-sectional area q, located at $x = \Delta$ (with $\Delta \to 0$).

Note that the impedances of the cold and hot regions have both been defined as positive in the $+x$ direction. The portion of the duct upstream of the temperature jump at $x = 0$—where heat is added—will be denoted region 1, with mean gas density ρ_1, mean temperature T_1 and sound speed c_1. Region 2 is downstream of $x = 0$, with gas density ρ_2, temperature T_2 and sound speed c_2. The inhomogeneous Helmholtz equation in region 2, which describes the pressure perturbation generated by the plane harmonic monopole source at $x = \Delta$, can be written as

$$\frac{\mathrm{d}^2 p}{\mathrm{d}x^2} + k_2^2 p = -i\omega\rho_2 q\delta(x - \Delta) \tag{1}$$

where $\delta(\ )$ denotes the Dirac delta function, p is the acoustic pressure and k is the acoustic wave number ($= \omega/c$). Integration of Eq. (1) w.r.t. x across the source plane and the use of the linearised Euler equation (for acoustic perturbations) together with the condition of continuity of sound pressure, give an expression for the jump in acoustic velocity across the source plane,

$$u_2(\Delta_+) - u_2(\Delta_-) = q, \tag{2}$$

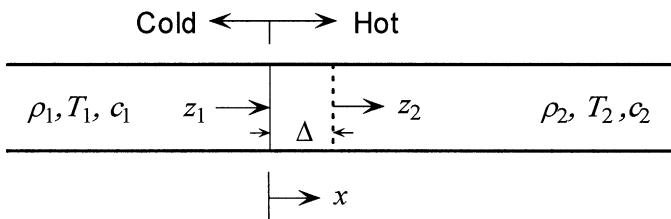consistent with the conservation of mass.

Fig. 2. A duct containing a slow gas flow with heat addition.

If it is assumed that $\Delta \to 0$, matching of particle velocity at $x = 0$ yields

$$u_2(\Delta_-) \underset{\Delta \to 0}{\to} u_2(0_+) = u_1(0_-). \qquad (3)$$

This would appear to be the correct kinematic boundary condition (which may also be found from the work of Rott [15], for a gas away from a solid boundary), corresponding to the position of the temperature jump being disturbed by the oscillating acoustic flow. Even if the temperature jump were stationary, however, this boundary condition would still apply, because of a stationary density fluctuation brought about by entropy fluctuations (see the paper by Dowling [16]). Impedances Z_1 and Z_2 may be defined as

$$Z_1 = p(\Delta)/u_1(0_-), \qquad (4)$$

$$Z_2 = p(\Delta)/u_2(\Delta_+), \qquad (5)$$

where $p_1 = p_2 = p$ (if $\Delta \to 0$) for $0 < x < \Delta$. Combining the above equations gives

$$q = p(\Delta)/Z_2 - p(\Delta)/Z_1 \qquad (6)$$

or

$$p(\Delta) = \frac{q}{1/Z_2 - 1/Z_1}. \qquad (7)$$

An impedance Z may be defined as $Z = p(\Delta)/q$, viz.

$$Z = \frac{1}{1/Z_2 - 1/Z_1}. \qquad (8)$$

This corresponds to an acoustic frequency response function (FRF) of the combustion system. If the impedances Z_1 and Z_2 can be calculated, then the pressure response of the system (Δp) to the flame oscillations (q) can be determined from Eq. (8).

4. A simple model for prediction of the impedances of the supply system and combustion chamber

Fig. 3 shows a schematic diagram of the combustion chamber divided into small elements. Both thermodynamic properties and cross-sectional area within a given section are assumed constant but may differ between sections. The sound field is assumed to be one-dimensional, in the axial direction, throughout. In practice, average values of thermodynamic properties (over the cross-section) may be taken as representative. At the interface separating the sections the condition of continuity of volume velocity may be taken to be the appropriate kinematic boundary condition and expressed in terms of acoustic particle velocity,
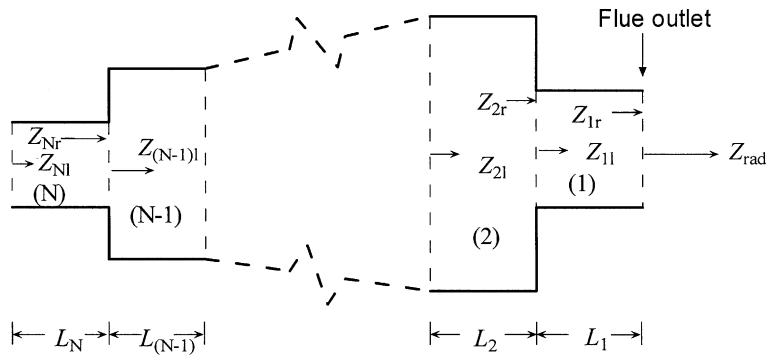
Fig. 3. A stepped model of a combustion chamber.

$$u_1 A_1 = u_2 A_2, \tag{9}$$

where A represents cross-sectional area, and continuity of sound pressure may be written

$$p_1 = p_2. \tag{10}$$

The impedances at the terminations of both the combustion chamber and the supply system must be specified. The radiation impedance of the flue termination was assigned the low-frequency limiting expression of an unflanged pipe found by Levine and Schwinger [17],

$$Z_{\text{rad}} = \rho \omega^2 R^2 / 4c + i0.61 R \rho \omega, \tag{11}$$

where R is the flue pipe radius. This is valid for a pipe of infinitesimal wall thickness and a homogeneous fluid. Alternatively, the experimental data of Cummings [18] for hot gas flow from an unflanged pipe could be used. The point at which the silencer connected to the settling chamber was modelled as a side-branch. The silencer was designed in order to give a specifiable upstream acoustic termination to the combustion system. Its impedance was predicted from

$$z = \rho_0 c_0 \left(\frac{1+r}{1-r} \right), \tag{12}$$

with reflection coefficient $r = \left(\dfrac{1 - k_x/k}{1 + k_x/k} \right),$ \hfill (13)

where ω is the radian frequency and k_x is the complex wave number, found from the expression of Cummings [19],

$$k_x = k \left(1 - \frac{2i}{k \zeta_w a} \right)^{1/2}. \tag{14}$$

Here, a is the silencer radius, k is the wave number and ζ_w is the dimensionless normal surface impedance of the sound absorbing material lining the silencer.

On the basis of the foregoing, standard acoustic transmission line theory—together with the matching conditions Eqs. (9) and (10)—may be used to predict the impedance of the combustion chamber by a "marching process" from right to left. This proceeds as follows:

$$Z_{1r} = Z_{\text{rad}} \tag{15}$$

(because of the continuity of particle velocity and sound pressure at the flue outlet),

$$Z_{1l} = \rho_1 c_1 \left[\frac{Z_{1r} + i\rho_1 c_1 \tan(k_1 L_1)}{\rho_1 c_1 + iZ_{1r} \tan(k_1 L_1)} \right], \tag{16}$$

$$Z_{2r} = \frac{Z_{1l} A_2}{A_1}, \tag{17}$$

$$Z_{2l} = \rho_2 c_2 \left[\frac{Z_{2r} + i\rho_2 c_2 \tan(k_2 L_2)}{\rho_2 c_2 + iZ_{2r} \tan(k_2 L_2)} \right] \tag{18}$$

and so on, until

$$Z_{Nl} = \rho_N c_N \left[\frac{Z_{Nr} + i\rho_N c_N \tan(k_N L_N)}{\rho_N c_N + iZ_{Nr} \tan(k_N L_N)} \right]. \tag{19}$$

In Eqs. (15)–(19), ρ_i, c_i and k_i are the gas density, sound speed and acoustic wavenumber in the ith section.

The above equations are the familiar relationships of acoustic transmission line theory. Knowledge of both the geometry of the system and the temperature distribution in the combustion chamber is required so that the cross-sectional areas, densities and sound speeds may be found.

5. Results and discussion

The impedances of the supply system and combustion chamber were predicted by using the method described in Section 4. Experimental measurements of the impedance of the supply system were taken by the use of a standing-wave tube. (This device is not restricted, in its application, to sound absorbing materials, as Cummings [20] commented: "There is..... no reason why it should not be used to measure the impedance of any conveniently sized sample".) Figs. 4 and 5 show a comparison between the predicted imaginary and real parts (respectively) of the impedance of the experimental supply system containing air under ambient conditions. Reasonable agreement between the two is noted, though the measured resis-
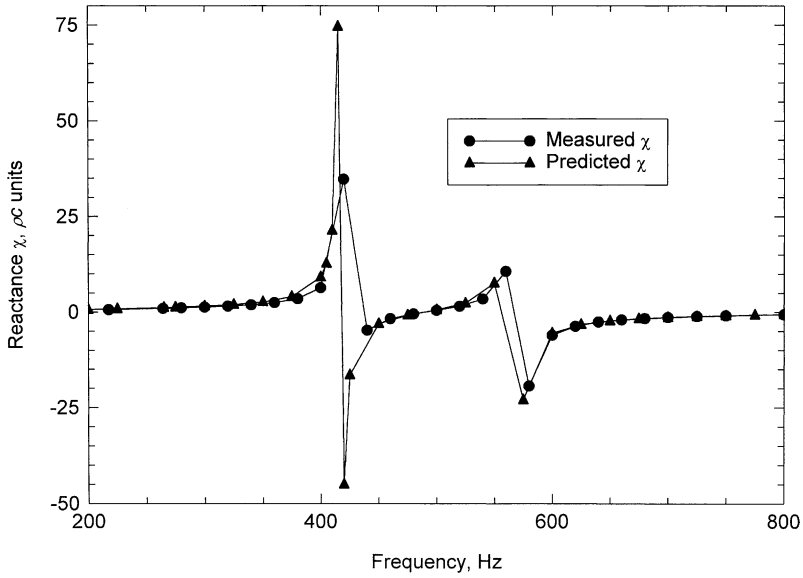
Fig. 4. Comparison between predicted and measured reactance of the supply system.
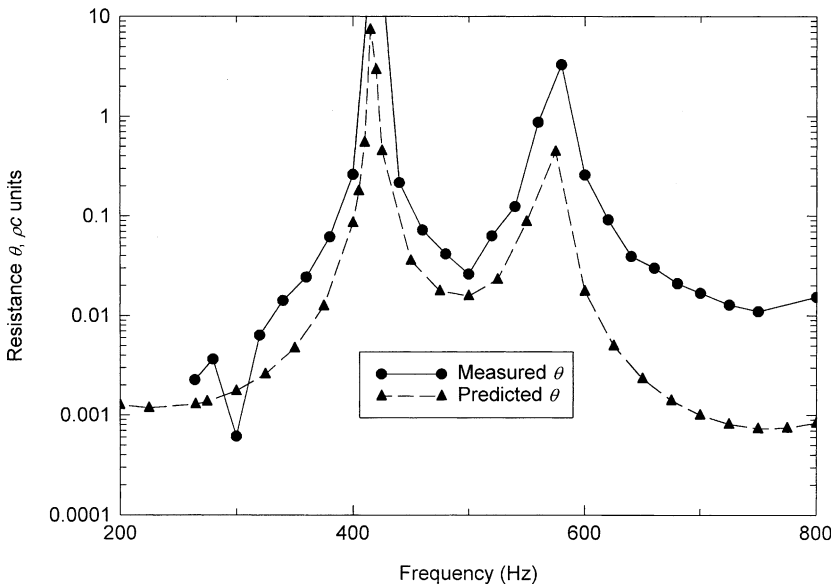

Fig. 5. Comparison between predicted and measured resistance of the supply system.

tance at the two antiresonances considerably exceeds the predicted values, probably because of losses not taken into account in the modelling (the disagreement at other frequencies is inconsequential—note the log scale for θ).

The combustion system was observed to exhibit oscillations when burning natural gas and air, for various combinations of the lengths of the combustion and settling chambers and within certain ranges of air/gas ratio. What appeared to be the second axial acoustic mode of the system was favoured and the frequency varied, depending on the operating conditions, but was usually rather less than 600 Hz. The full range of operating conditions was covered in the experimental tests, and instability plots were drawn for different combination of combustion and settling chamber lengths. Fig. 6 shows a typical plot of the instability envelope of the combustion system with the dimensions shown in Fig. 1. Oscillation frequencies are also shown here. The independent variables are air and gas volume flow rates. As is quite common with combustion oscillations, the instability region centres around the stoichiometric air/gas ratio (with "equivalence ratio" $\phi = 1$), and has a lower bound in terms of gas flow rate. Immediately after ignition the system started to oscillate, and showed a substantial region of instability. The frequency of oscillations tended to increase as the mixture flow rate was increased, mainly because of the increase in temperature within the combustion chamber. In order to verify the one-dimensional nature of the sound field and confirm the order of the acoustic mode at the oscillation frequency, both the frequency response function (FRF) of the system to a random noise signal and the axial sound pressure distribution within the system, at a discrete frequency, were measured. (The FRF represents the ratio between the sound pressure at a given point in the system and the volume velocity of a monopole source at a specified
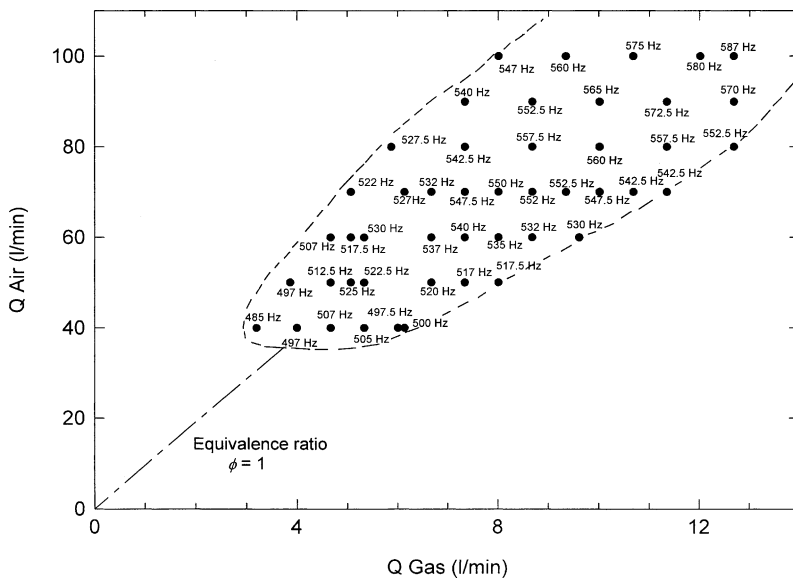

Fig. 6. Instability plot for the experimental combustion system.

point, both quantities being defined in the frequency domain.) Both these tests were conducted with the system initially at ambient temperature, without combustion, and then in the "hot" system, only the axial sound pressure distribution was measured as the system exhibited autonomous oscillations.

The FRF tests in the cold system involved a small source loudspeaker with a backing enclosure, which was positioned in the combustion chamber close to the burner head and fed with a random noise signal. The acoustic response of the system was detected by the use of a microphone, placed near the burner head at the same axial location as the loudspeaker. Peaks in the spectrum of the sound pressure correspond to eigen-frequencies of the burner system [see Eq. (8)].

Fig. 7 shows a comparison between the measured resonance frequencies of the cold combustion system and a plot of |Z|. It can be seen that very good agreement between predicted and measured oscillation frequencies of the cold combustion system is obtained by using the one-dimensional model described above. At the second mode resonance frequency of the cold combustion system (385 Hz) a steady sinusoidal signal was fed to the loudspeaker to permit investigation of the sound pressure distribution in the cold combustion. Fig. 8 shows a comparison between the predicted and measured sound pressure level (L_p) patterns in the cold system. A well-defined pressure node is noted at about 0.4 m from the top of the burner. In a similar way the sound pressure distribution in the hot combustion system was predicted and measured at the frequency of autonomous oscillations. Fig. 9 shows comparison between the measured and predicted sound pressure patterns in the hot combustion system, with the specified flow rates of air and gas, as it underwent
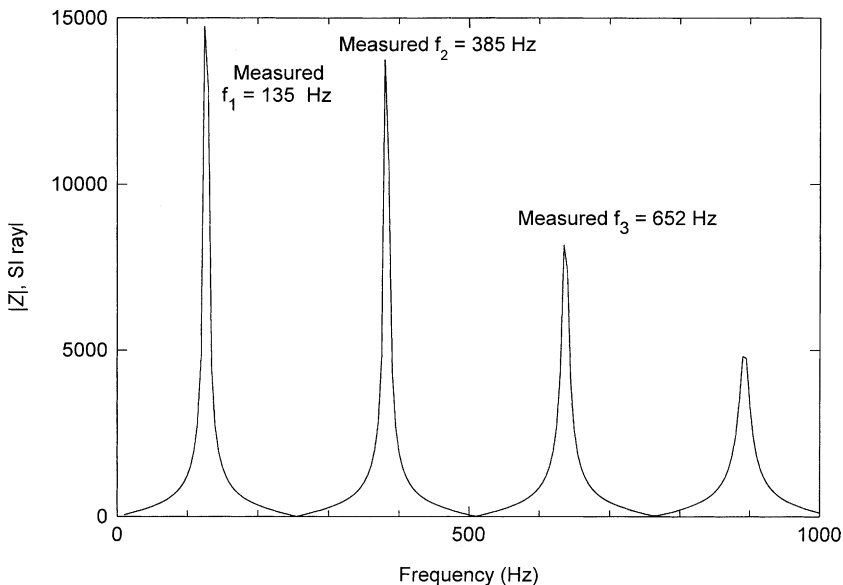

Fig. 7. Predicted magnitude of impedance in the cold system and measured peak frequencies in the FRF spectrum.
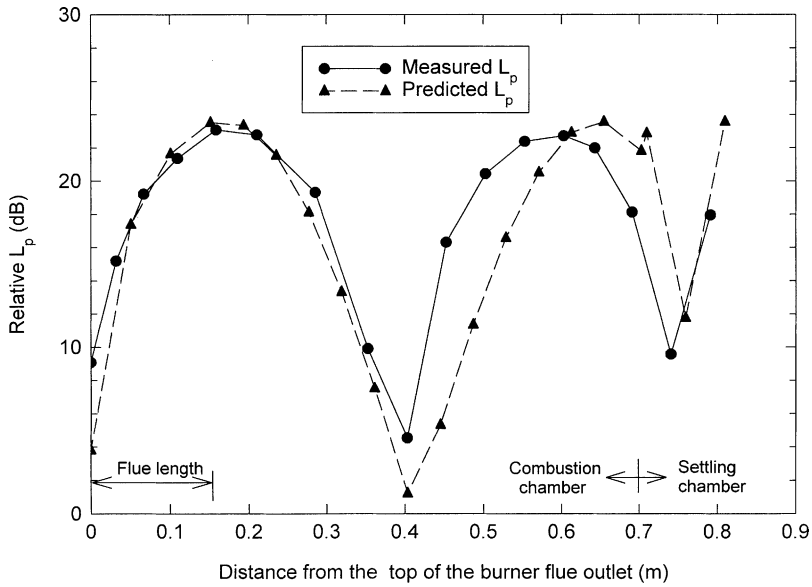
M. Elsari, A. Cummings / Applied Acoustics □ (□□□□) □–□

Fig. 8. Measured and predicted acoustic pressure patterns in the cold combustion system at 300 K obtained by injecting a signal at $f = 385$ Hz.
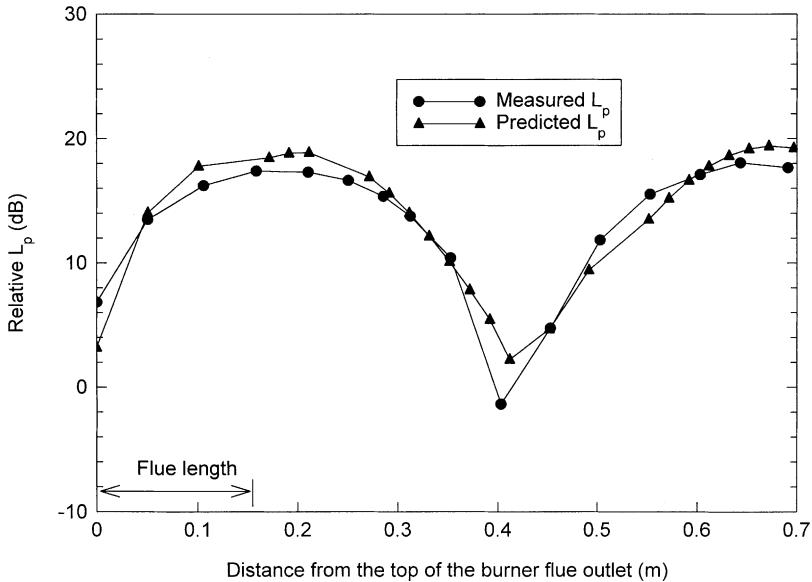

Fig. 9. Measured and predicted acoustic pressure patterns in the combustion chamber with the burner operating, at the oscillation frequency, with flow rates of 50 l/min air and 5.87 l/min gas.

M. Elsari, A. Cummings / Applied Acoustics □ (□□□□) □–□ 13

autonomous oscillation. At this frequency (522 Hz), higher acoustic modes could not propagate, and it was therefore concluded that an axially-propagating second mode ''resonance'' was being driven by the unsteady combustion process. It is worth nothing that the burner plate (0.7 m from the flue outlet) is located near a sound pressure antinode.

These observations are—to some extent—consistent with Rayleigh's Criterion [3], ''*if heat be periodically communicated to, and abstracted from, a mass of air vibrating (for example) in a cylinder bounded by a piston, the effect produced will depend upon the phase of the vibration at which the transfer of heat takes place. If heat be given to the air at the moment of greatest condensation, or taken from it at the moment of greatest rarefaction, the vibration is encouraged. On the other hand, if heat be given at the moment of greatest rarefaction, or abstracted at the moment of greatest condensation, the vibration is discouraged.*'' Apart from the phase criterion, there is also a requirement that heat should be added at a point where the sound pressure varies significantly, and the acoustic mode will be most strongly driven when the heat release takes place at or near a pressure antinode.

Fig. 10 shows the computed modulus of the impedance at the flame in the hot system, [see Eq. (8)], plotted as a function of frequency. The predicted curve peaks close to the measured second mode frequency (522 Hz) of the combustion system evident in the frequency spectrum shown in Fig. 11, which was taken with the hot combustion system operating with the same flow rates of air and gas as those of Fig. 10. The predicted peaks in Fig. 10 correspond to eigenmodes of the hot combustion system. The agreement between prediction and measurement is good but not
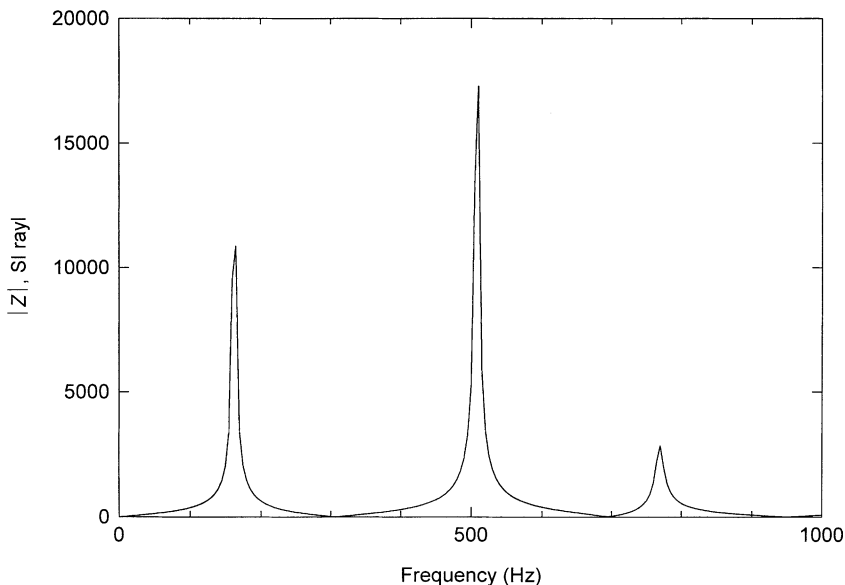

Fig. 10. Predicted magnitude of impedance in the hot combustion system with flow rates of 50 l/min air and 5.87 l/min gas.

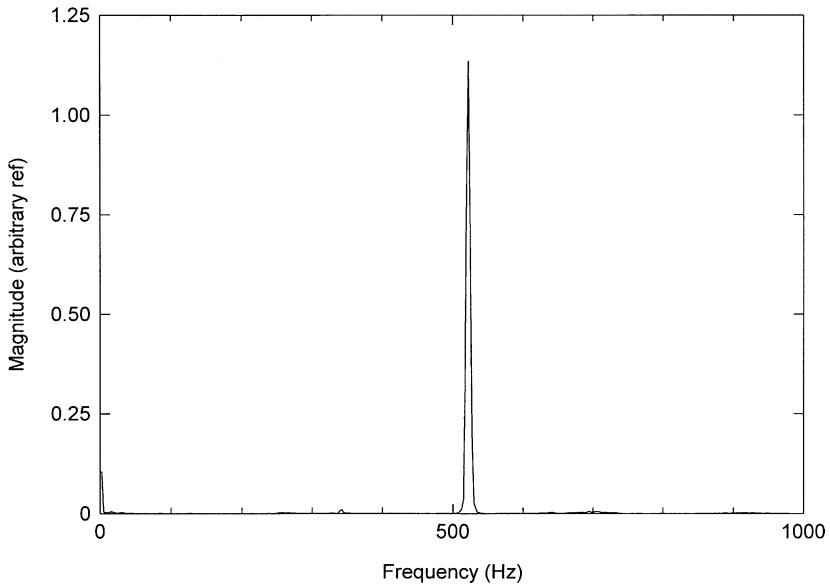14   *M. Elsari, A. Cummings / Applied Acoustics □ (□□□□) □–□*

Fig. 11. Typical measured frequency spectrum of oscillations of the hot combustion system with flow rates of 50 l/min air and 5.87 l/min gas.
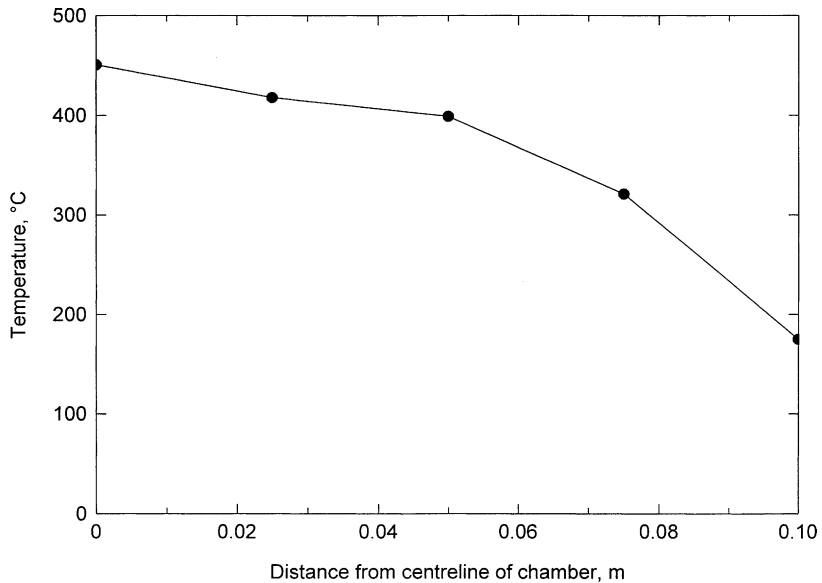

Fig. 12. Transverse temperature distribution on a typical cross-section of the hot combustion system, in a central plane parallel to the walls.

perfect, partly because the measured temperature data were not completely representative of the effective temperature, averaged over the cross-section of the combustion chamber. Fig. 12 shows the temperature distribution in a typical cross-section of the combustion chamber. Large transverse temperature gradients existed, particularly near the walls, and these could in principle lead to some uncertainty in the wave propagation speed. However, measured sound pressure data on a typical cross section suggest that the sound pressure profile of the wave is actually fairly uniform. A further point is that the flame has been regarded as a simple volume source and this approximation, too, could perhaps bring about some inaccuracy in frequency prediction since a highly complex feedback mechanism is actually involved. At all events, the agreement between the predicted and measured oscillation frequency is fairly good, and offers convincing evidence that it is an acoustic mode of the whole combustion system that is being driven by the flame oscillations.

6. Conclusions

This research shows that the acoustics of the combustion system can be adequately represented by the use of a simple one-dimensional model, which gives fairly good predictions of the frequency of oscillations and of the sound field in the system. Because the flame dynamics were not included in the model, the prediction of instability regimes was not possible. However, since the main objective of this work is to investigate the use of passive devices to suppress combustion oscillations, the acoustic model is, in itself, a useful design tool which can be used to determine the optimum location of these devices. In future work, acoustic modelling of the system should be combined with research on flame dynamics in an effort to predict instability regimes in the entire system.

Acknowledgements

References

[1] Higgins B. On the sound produced by a current of hydrogen gas passing through a tube [by the editor, Mr. Nicholson, with a letter from Dr. Higgins respecting the time of its discovery]. J Nat Philos Chem, Arts 1802;1:129.
[2] Putnam AA. Combustion driven oscillations in industry. New York: American Elsevier; 1971.
[3] Lord Rayleigh (J.W. Strutt). The theory of sound, vol. 2. New York: Dover; 1945. p. 226.
[4] Candel SM, Poinsot TJ. Interaction between acoustics and combustion. Proceeding of the Institute of Acoustics 1988;10:103.

16 *M. Elsari, A. Cummings / Applied Acoustics □ (□□□□) □–□*

[5] Yang V, Anderson E. Liquid rocket engine combustion instability. Progress in Astronautics and Aeronautics 1995;169:358.

[6] Dowling AP, Bloxsidge GJ. Reheat buzz—an acoustically driven combustion instability. Ninth AIAA Aeroacoustics Conference, Paper 84-2321, 1984.

[7] Tsuji H, Takeno T. An experimental investigation on high-frequency combustion oscillations. In: Tenth Symposium (International) on Combustion, 1965. p. 1327.

[8] Carvalho JA, Wang MR, Miller N, Daniel BR, Zinn BT. Controlling mechanisms and performance of coal burning Rijke type pulsating combustors. In: Twentieth Symposium (International) on Combustion, 1984. p. 2011.

[9] Schimmer H, Vortmeyer D. Acoustical oscillations in a combustion system with a flat flame. Combustion and Flame 1977;28:17.

[10] Putnam AA, Dennis WR. Organ-pipe oscillations in a burner with deep ports. Journal of the Acoustical Society of America 1956;28:260.

[11] Janardan BA, Daniel BR, Zinn BT. Driving of combustor oscillations by gaseous propellant injectors. In: Seventeen Symposium (International) on Combustion, 1978. p. 1353.

[12] Chen TY, Chen MG. Sound emission of ducted premixed flames. Journal of Sound and Vibration 1999;221:221.

[13] Mugridge BD. Combustion driven oscillations. Journal of Sound and Vibration 1980;70:437.

[14] Merk HJ. An analysis of unstable combustion of premixed gases. In: Sixth Symposium (International) on Combustion, 1957. p. 500.

[15] Rott N. Damped and thermally driven oscillations in wide and narrow tubes. ZAMP 1969;20:230.

[16] Dowling AP. The calculation of thermoacoustic oscillations. Journal of Sound and Vibration 1995;180:557.

[17] Levine H, Schwinger J. On the radiation of sound from an unflanged circular pipe. Physical Review 1948;73:383.

[18] Cummings A. High temperature effects on the radiation impedance of an unflanged duct exit. Journal of Sound and Vibration 1977;52:299.

[19] Cummings A. Low frequency acoustic transmission through the walls of rectangular ducts. Journal of Sound and Vibration 1978;61:327.

[20] Cummings A. Measurement of the acoustic impedance of gas burners using a standing wave tube [internal report no. I699]. The Gas Council Midlands Research Station, September 1971.